

REFRACTIVE INDICES OF CASSITERITE

By

STEINAR SEI-HWA HUANG

Bachelor of Science

University of Wyoming

Laramie, Wyoming

1958

Submitted to the Faculty of the Graduate School of
the Oklahoma State University

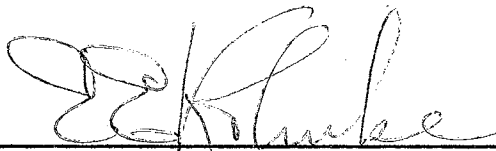
in partial fulfillment of the requirements
for the degree of
MASTER OF SCIENCE

May, 1963

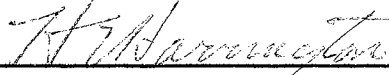
JAN 7 1964

REFRACTIVE INDICES OF CASSITERITE

Thesis Approved:



Thesis Adviser



Dean of the Graduate School

541987

ACKNOWLEDGEMENT

I wish to express the deepest and most sincere gratitude to my adviser, Dr. E. E. Kohnke for his patience and valuable guidance throughout the course of this research. I also would like to thank Dr. H. E. Stocking of the Geology Department for his help in determining the optic axis of the crystal. Special thanks also goes to Dr. H. P. Hotz for his suggestions and to Professor F. Harris for his loan of spectral lamps.

To the personnel of the machine shop I wish to thank H. Hall for his cutting and polishing of the prism and to F. Hargrove for constructing most of the mirror spectrograph.

Last but certainly not least I wish to express my deepest thanks to my wife, Tai-Bieng, for her patience and understanding during the completion of this work and I would also like to thank her for translating a German reference article.

TABLE OF CONTENTS

Chapter	Page
I. INTRODUCTION.	1
II. THEORETICAL DISCUSSION.	4
Crystal Structure of Cassiterite	4
Birefringence.	11
Dispersion	16
III. DISPERSION MEASUREMENT.	21
Cutting and Polishing of the Prism	21
Experimental Procedures.	23
Derivation of the Formula Used in Calculating the Refractive Indices with Data Obtained by the Mirror Spectrograph	24
Description of Spectroscopic Plates.	29
IV. RESULT OF MEASUREMENT AND ITS ACCURACY.	31
V. SUMMARY AND CONCLUSION.	38
Brief Summary of the Work.	38
Conclusions.	39
Suggestions for Further Study.	40
BIBLIOGRAPHY	42

LIST OF TABLES

Table	Page
I. Exposure Time	30
II. Refractive Indices	32
III. Relative Differences of the Refractive Indices	34

LIST OF FIGURES

Figure	Page
1. Tetragonal Crystal Axes	7
2. Symmetry Planes	7
3. First Order Dipyrarnid	7
4. Second Order Dipyrarnid.	7
5. Five Possible Cross-Sections of Ditetragonal Dipyrarnid. .	7
6. Ditetragonal Dipyrarnid.	7
7. Cassiterite Twin.	10
8. Negative Uniaxial Crystal	12
9. Positive Uniaxial Crystal	12
10. Ray Direction and Wave Normal Direction of a Uniaxial Crystal	13
11. Huygen's Construction for the Ordinary and the Extraordinary Rays in a Uniaxial Crystal (The Optic Axis is in the Plane of the Figure)	14
12. Ordinary and Extraordinary Rays in a Uniaxial Crystal with the Optic Axis Perpendicular to the Plane of the Incidence	15
13. A Uniaxial Interference Figure Looking Down An Optic Axis.	22
14. Schematic Diagram of the Mirror Spectrograph.	26
15. Ray Diagram	26
16. Dispersion Curve.	36

CHAPTER I

INTRODUCTION

The semiconducting properties of many oxides have been studied. Northrip (1) and Hurt (2) made a rather comprehensive survey of the published works on tin oxide and titanium oxide, the latter being the prototype rutile-structure material.

Little has been done with cassiterite. Investigation has just begun in recent years on its optical and electrical properties. Northrip conducted optical measurements on several natural cassiterite crystals. He found the short wavelength cutoff in the region of 0.350 - 0.360 microns and an intense absorption in the region of 3.1 microns.

DC and AC photoconductivity measurements were taken by Hurt, with variations of sensitivity with changes in the wavelength and intensity of the incident light as well as the influence of temperature and prolonged exposure to light on the photoconductive behavior studied most extensively.

Optical transmission measurements on natural crystals of cassiterite in the region from the short wavelength cutoff to 4.0 microns at three different temperatures were made by Belski (3). Certain samples used by Belski had undergone special oxidation or reduction treatment. A room temperature value of 3.47 eV was obtained for the optical forbidden gap. The absorption edge also showed a shift with temperature. The 3.1 micron absorption band was attributed to O-H stretching vibrations. An apparent shift of the band toward shorter wavelength with decreasing temperature

was also observed.

Reproducible Hall coefficient data which allowed calculation of the number of charge carriers taking part in the conduction process and their mobilities over an as yet restricted temperature range was obtained by Tolly (4).

Ohmic contacts were made by Houston (5) to cassiterite for making field effect measurements by a beat frequency bridge method.

The attempts to grow stannic oxide crystals by hydrothermal methods have failed (6), however, small stannic oxide crystals of size up to 10 X 0.1 X 0.1 mm have been grown from the melt. Single crystals of stannic oxide up to 30 X 4 X 2 mm have been prepared by a high temperature vapor deposition technique at Corning Glass Works by Marley and MacAvoy (7).

A survey of the results on natural crystals to date has been given by Kohnke (8).

The technique of growing single crystals of stannic oxide needs to be improved so that larger sizes will be available for cutting properly orientated prisms for dispersion study. Both Ecklebe (9) and the author obtained their prisms from natural cassiterite ore from Araca, Bolivia.

Ecklebe's room temperature dispersion measurements of cassiterite only covered the visible spectrum. For the ordinary ray the range was from 423.1 to 715.2 millimicrons and for the extraordinary ray the range was from 444.0 to 715.2 millimicrons.

Since the short wavelength cutoff was found to be between 350 to 360 millimicrons, it is the purpose of this work to not only check Ecklebe's measurements in the visible spectrum but also to extend measurements as close to the cutoff as possible. Measurements in the ultra-violet require the use of photographic plates and a mirror spectrograph

which does not have any component that will absorb ultraviolet radiation. Also in order to obtain dispersion measurements both for the ordinary ray and the extraordinary ray, the prism should be cut so that the optic axis of the crystal lies in the refracting edge of the prism.

Extending dispersion measurements to close to the cutoff was desired to provide better data for reflection corrections in computing the absorption coefficient.

Dichroism had been observed in cassiterite, with the absorption of the extraordinary ray greater than that of the ordinary ray (10). It is also a purpose of this study to verify this fact.

CHAPTER II

THEORETICAL DISCUSSION

Crystal Structure of Cassiterite

The following brief discussion of the crystal structure of cassiterite has been compiled from text book sources on mineralogy, principally those of Hurlbut (11) and Buerger (12).

The most important ore of tin is the tin oxide, cassiterite, known commonly as tinstone. The geologist knows the mineral by the name of stream tin or wood tin. Stream tin is the name applied to cassiterite found in placers and wood tin is a variety of cassiterite having a fibrous structure. It should be mentioned here that stannite (tin pyrites) is a complex sulphide of copper, iron, and tin.

The two minerals of tin, cassiterite and stannite, are found in veins cutting granite and rhyolites, which have generally been greatly altered as the result of pneumatolytic action. Both stannite and cassiterite are resistant to weathering and accumulate as residual deposits at the outcrops of veins and in placers derived from them. Cassiterite may also occur as a primary constituent of pegmatic dikes, associated with lithium and phosphorous minerals, as near Gaffney, South Carolina, or in the Black Hills, South Dakota. These dikes exhibit sharp walls, and there is no replacement of the wall rock by cassiterite.

The pure mineral of cassiterite contains about 78.8 per cent tin.

It is a heavy, insoluble mineral that lacks the metallic luster of many ores. Specific gravity is 6.8 to 7.0. Hardness is 6 to 7. Luster is adamantine, and crystals are usually splendid; color is brown or black, sometimes red, gray, white, or yellow. Streak is white, grayish, or brownish. Cleavage is practically non-existent. Fracture is sub-conchoidal to uneven.

X-ray study shows for cassiterite an atomic structure in which the tin atoms are arranged on a body-centered tetragonal lattice. The oxygen atoms lie in the same horizontal planes as the tin atoms, and are grouped in pairs about each tin atom. Lines joining the pairs of oxygen atoms have the direction of one or the other of the prism diagonals and alternate in direction in each successive horizontal atomic layer.

Cassiterite belongs to the ditetragonal dipyramidal class with symmetry of $4/m$, $2/m$, $2/m$ of the tetragonal system. Crystals are usually short prismatic, showing the prisms and dipyramids of the first and second order. Twins are common--both contact twins and penetration twins--the dipyramid of the second order being the twinning plane.

The tetragonal system includes all crystals which can be referred to three perpendicular axes, two of which are equal and lie in a horizontal plane. These are termed the lateral axes and are designated as the a-axes. Perpendicular to the plane of the lateral axes is the principal or c-axis, which may be longer or shorter than the a-axes. The axes which bisect the angles between the a-axes are the intermediate axes. They are designated as the b-axes in Figure 1.

For crystals of the tetragonal system the unit lengths of a- and c-axes are unequal. The ratio between these unit lengths is the axial ratio, $a:c$.

The ratio between the lengths of the axes of crystals of a given substance is constant. In the hexagonal and tetragonal systems the lengths of vertical c-axes differ from those of the lateral a-axes, which are equal. In each of these systems the length of the c-axis to that of a-axis is characteristic for each substance crystallizing in the system.

There are five planes of symmetry in ditetragonal dipyramidal class. The plane of the lateral and the intermediate axes is termed the horizontal axial or principal (h) plane. The vertical planes including the c-axis and one of the a-axes are called the vertical axial (a) planes, while those which include one of the b-axes are termed the intermediate planes.

The three axial planes divide space into eight equal parts, termed octants, while the five planes divide it into sixteen equal sections as shown in Figure 2.

The c-axis is an axis of fourfold symmetry. The lateral and intermediate axes possess two fold symmetry. A center of symmetry is also present in this class.

The tetragonal dipyramid of the first order is analogous to the octahedron of cubic system; which has ratios of (a:a:a); but since the c-axis differs from the lateral axes, the ratio must be written (a:a:c), which would indicate the cutting of all three axes at unit distances as shown in Figure 3. As the intercept along the c-axis in general may be longer or shorter than the unit length, the general symbols would be (a:a:mc) or (hhl), where m is some rational value between zero and infinity. Like the octahedron, this form the tetragonal dipyramid, is bounded by eight faces which enclose space. The faces are equal isosceles triangles when the development is ideal.

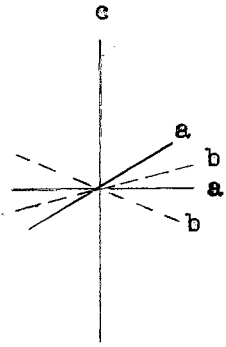


Figure 1
Tetragonal Crystal Axes

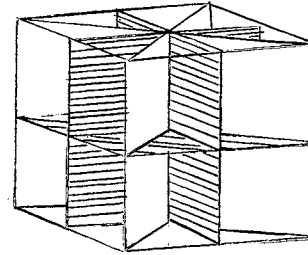


Figure 2
Symmetry Planes

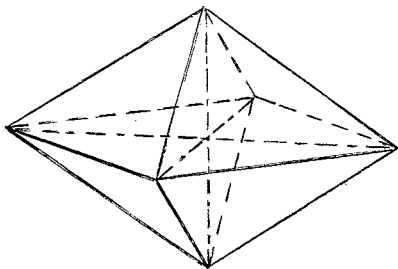


Figure 3
First Order Dipyramid

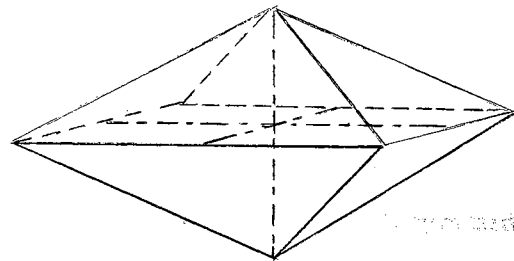


Figure 4
Second Order Dipyramid

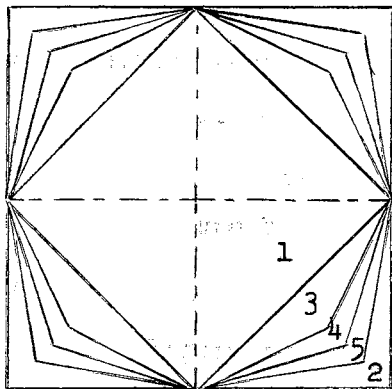


Figure 5
Five Possible Cross-Sections of
Ditetragonal Dipyramid

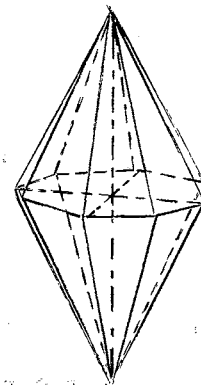


Figure 6
Ditetragonal Dipyramid

The principal crystallographic axis passes through the two tetrahedral angles of the same size, the lateral axes through the other four equal tetrahedral angles, while the intermediate axes bisect the horizontal edges.

The tetragonal dipyramid of the second order in Figure 4 is very similar to the preceding, but can be readily distinguished from it due to its position with respect to the lateral axes. In this form, the lateral axes bisect the horizontal edges while the intermediate axes pass through the four equal tetrahedral angles. This is the opposite of what was noted with the dipyramid of the first order. Hence, the dipyramid of the first order is always held so that an edge is directed toward the observer, whereas the dipyramid of the second order presents a face. In both dipyramids the principal axis passes through the two equal tetrahedral angles.

The faces of this form cut the c-axis and one of the a-axes but extend parallel to the other. The symbols are, therefore, $(a:\infty a:mc)$ or $(h0l)$. Eight faces are required to enclose space and the form is termed dipyramid of the second order.

The faces of the ditetragonal dipyramid cut the two lateral axes at different distances, while the intercept along the c-axis may be unity or mc. Sixteen such faces are possible and hence the term ditetragonal dipyramid is used (see Figure 5). The symbols are: $(a:na:mc)$ or (hkl) . Since the polar edges are alternately similar, it follows that the faces are equal, similar scalene triangles. The ditetragonal dipyramid possessing equal polar edges is crystallographically an impossible form, for then the ratio $a:na:mc$ would necessitate a value for n equal to the tangent of $67^{\circ}30'$, namely, the irrational value of 2.4142+.

From the above paragraph it follows that, when n is less than $2.4142+$ the ditetragonal dipyramid simulates the tetragonal dipyramid of the first order, and finally, when it equals 1, it passes over into that form. On the other hand, if n is greater than $2.4142+$, it approaches more the dipyramid of the second order, and when it is equal to infinity passes over into that form, hence, $1 < n < \infty$. It is also to be noted that when n is less than $2.4142+$, the lateral axes pass through the more acute angles, whereas, where n is greater than $2.4142+$ they join the more obtuse. Outline 1 of Figure 5 represents the cross section of the tetragonal dipyramid of the first order, 2 that of the second order, and 3, 4, and 5 the cross section of ditetragonal dipyramid, where n equals $3/2$, 3, and 6, respectively. See Figure 6 for an example of a ditetragonal dipyramid. Common forms of cassiterite are prisms and dipyramids of first and second order.

Crystals of a single species frequently grow in positions in which the parallelism of the parts is incomplete; that is, some corresponding directions are exactly parallel and others are not. Two crystals of the same kind, which form an aggregate exhibiting such partial parallelism, are called a twin, or are said to be in twinning position. The relative position of two crystals in twinning position may be most readily understood by assuming that one has been revolved through 180° about some direction or axis, which thus remains common to both. It should be emphasized that twins are not produced by such a revolution, but by regular growth (except the secondary twins produced by shearing or stresses); this is merely a convenient way to describe the relative positions.

The axis about which one part is supposed to be revolved is called

the twinning axis, and the plane normal to this is the twinning plane. The plane by which twinned crystals are united is called the composition plane. This is often the same as the twinning plane, but it is not necessarily so; when it is not the same as the twinning plane, the composition plane is apt to be parallel with the twinning axis. The twinning axis is nearly always a crystal axis or normal to a possible crystal face. If twins are simply adherent by the composition face, they are contact twins; if they interpenetrate more or less, they commonly have an irregular composition surface and are called penetration twins. In many cases twins are composed of more than two parts, the mutual relations of any two adjacent parts being the same. In this case the twinning is described as multiple or polysynthetic, if the composition faces are parallel, and cyclic or symmetrical, if the composition faces are not parallel and therefore tend to turn in a circle. Repeated twinning of the cyclic type often gives rise to an apparent symmetry, called pseudosymmetry, greater than that actually possessed by the crystal. Twinning may be produced artificially, in some cases, by shearing or other stresses; such twinning is called secondary. Figure 7 shows the form of a cassiterite twin, comparable to the original crystal from which the experimental prism was cut.

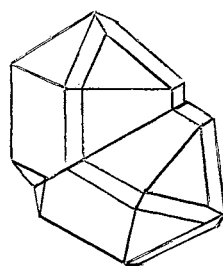


Figure 7: Cassiterite Twin

Birefringence

When a beam of unpolarized light is incident on a calcite or any uniaxial anisotropic crystal, there will be the reflected beam and two refracted beams instead of the usual single refracted beam observed as in an isotropic medium, e.g. glass. This phenomenon is called double refraction. It is found that Snell's law of refraction holds for one beam but not the other. The beam for which Snell's law applies is called the ordinary ray (o-ray), the other, the extraordinary ray (e-ray).

This phenomenon was observed by Huygens in 1670 and the remarkably simple explanation given below for the phenomenon of double refraction in a uniaxial, anisotropic crystal is due to him (13).

Since the o-ray always lies in the plane of incidence and obeys Snell's law, Huygens suggested that it is propagated as a spherical wave. He next assumed that the e-ray propagated as an ellipsoidal wave, its wave front being an ellipsoid of revolution formed by rotating an ellipse about one of its principal axes. This choice was due to the fact that an ellipsoid is the next simplest geometrical form.

In a uniaxial crystal, such as cassiterite, the optic axis is the line joining the two points at which the sphere and ellipsoid of revolution touch. There are two possible cases:

Case I) Negative uniaxial crystal (e.g. Calcite)

The sphere is inside the ellipsoid of revolution, and a section is shown in Figure 8. The e-ray propagates faster than the o-ray except along the optic axis A'A where both rays propagate at the same speed. This is due to the fact that when the o-ray reaches any point B on the sphere from a source O inside the

crystal, the e-ray has already reached point B' on the ellipsoid and $OB' > OB$. If the length of the long and the short semi-axes of the ellipsoid are denoted by 'a' and 'b' respectively, the equations of the section are:

$$\text{ellipse} \quad y^2/a^2 + x^2/b^2 = 1 \quad (1)$$

$$\text{circle} \quad x^2 + y^2 = b^2 \quad (2)$$

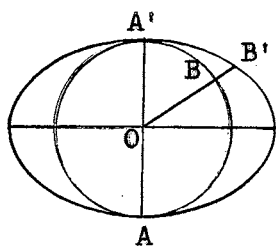


Figure 8

Negative Uniaxial Crystal

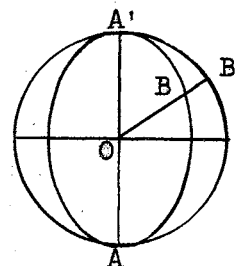


Figure 9

Positive Uniaxial Crystal

Case II) Positive uniaxial crystal (e.g. Cassiterite)

The ellipsoid of revolution is inside the sphere. The equations of the section shown in Figure 9 are:

$$\text{ellipse} \quad x^2/a^2 + y^2/b^2 = 1 \quad (3)$$

$$\text{circle} \quad x^2 + y^2 = a^2 \quad (4)$$

The o-ray now propagates faster than e-ray except in the direction of optic axis where both rays propagate at the same speed.

In the case of positive crystal the ellipsoid is prolate, in the negative crystal it is oblate when referred to the optic axis direction.

It should be mentioned here that in a uniaxial crystal, the optic axis in the trigonal, tetragonal and hexagonal crystals coincides with the crystallographic c-axis.

The electric field vibrations are always in the wave front. In the o-ray, the wave front is a tangent plane to the sphere and since this is

always perpendicular to the radius of the sphere, which is the direction of the ray, the vibrations in the o-ray are always perpendicular to the ray. The wave front of an e-ray is a tangent plane to the ellipsoid; this tangent plane is not in general perpendicular to the radius vector OB' , and hence the vibrations in the e-ray are not perpendicular to the ray, unless this is in the direction of an optic axis. In Figure 10 the wave direction is shown joining the center of the ellipsoid to the point of contact of the tangent plane, while the wave normal is perpendicular to the latter. The ray gives the direction in which the energy of the light travels in the crystal.

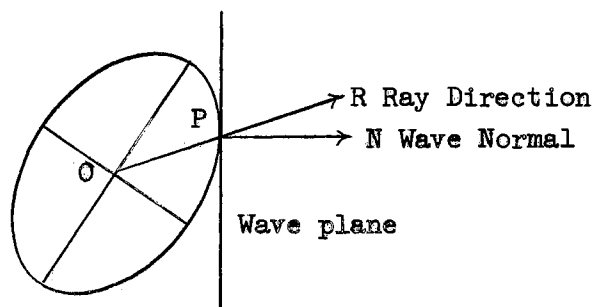


Figure 10

Ray Direction and Wave Normal Direction of a Uniaxial Crystal

Consider a uniaxial crystal with the optic axis in the plane of the paper. The wave front of the o-ray is found by Huygens' construction, viz. by drawing a tangent plane to the spherical wavelets diverging from the points of incidence. The spherical wavelet generated when the wave front AB of the incident ray reaches A is shown in Figure 11. When it has spread in the crystal to the position shown, a following wave is incident at A' , and all the intervening waves would have generated spherical wavelets of diminishing size between A and A' . Since the wavelet at A' has only just begun to spread, it is represented by a point.

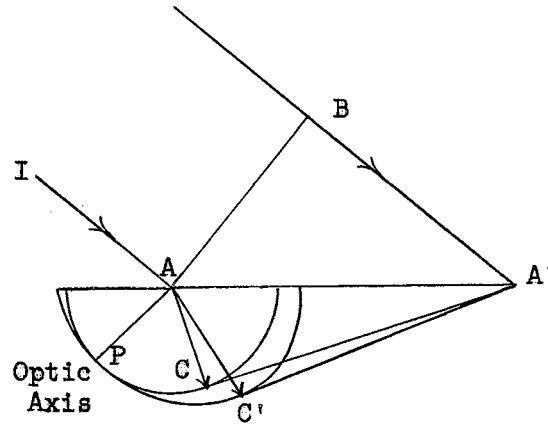


Figure 11

Huygen's Construction for the Ordinary and the Extraordinary Rays in a Uniaxial Crystal (The Optic Axis is in the Plane of the Figure)

The tangent plane AC will touch all the spherical wavelets between A' and that shown diverging from A, and these need not be drawn. The e-ray wavelets spread as spheroids, touching the sphere on the optic axis, which in this case is assumed to be in the plane of the paper. The tangent plane A'C' to the spheroid is the wave front of the e-ray. Hence AC and AC' are the ordinary and the extraordinary ray directions. It should be noted that these will not be in the same plane unless the optic axis lies in the plane of incidence or is perpendicular to the plane of incidence. In the described case, they are in the same plane.

When the optic axis is perpendicular to the plane of incidence, the sections of the sphere and spheroid, at right angles to the optic axis, are concentric circles and the two rays are in the plane of the paper as shown in Figure 12.

If the velocity in air is unity and the equivalent velocities of the ordinary ray and extraordinary ray are b and a , in the proportion of the radii of the circles, then the refractive indices have the following forms. If i is the angle of incidence, r_o and r_e the angles of refraction for the ordinary and the extraordinary rays, then:

$$n_o = \sin i / \sin r_o = 1/b \quad (5)$$

$$n_e = \sin i / \sin r_e = 1/a \quad (6)$$

A uniaxial crystal has two refractive indices for every incident ray direction. One of these, n_o , is constant for all ray directions. The other, n_e , varies with the ray direction, but its value is taken when this direction is perpendicular to the optic axis. In this case the incident and extraordinary rays lie in the same plane and Snell's law applies, $\sin i / \sin r$ being constant for various values of i less than the critical angle.

For the situation where the optic axis neither lies in, or perpendicular to, the plane of incidence, the Huygens' construction is more complicated but the same principles apply. As will be seen later, the case described in Figure 12 is the one which applies to the experimental measurements reported here.

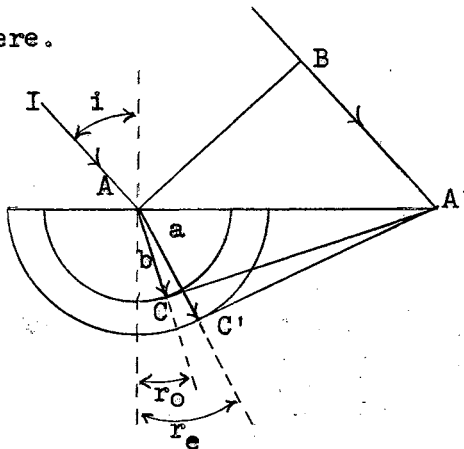


Figure 12

Ordinary and Extraordinary Rays in a Uniaxial Crystal with the Optic Axis Perpendicular to the Plane of the Incidence

Dispersion

The phenomenon that involves the interaction of a light wave with the electric charges in a substance is called dispersion. Basically this interaction leads to a variation of the index of refraction with the wavelength of the incident light. Using classical concepts of the behavior of oscillating charges, the phenomenon of scattering leads to a physical interpretation of dispersion. Briefly, the light scattered by the individual bound charges of a substance interferes in the forward direction with the primary wave to produce a phase change in it. This change in phase manifests itself as a change in the phase or wave velocity. Since the phase of the scattered waves varies with the frequency of the incident radiation, there results a change in velocity with frequency as the light wave enters a refracting medium (13).

The development of the theory of dispersion has been by a series of successively more general treatments satisfying the experimental data of the time (14).

(1) In 1836 Cauchy found an empirical equation for the dependence of the index of refraction n on wavelength λ for substances that are transparent over the visible range of the spectrum. The Cauchy dispersion formula is

$$n = A + B/\lambda^2 + C/\lambda^4 \quad (7)$$

where A , B and C are different constants for any one substance. Often it is sufficient to use the Cauchy formula with only two constants, the λ^4 term being neglected. Thus

$$n = A + B/\lambda^2 \quad (8)$$

Hartmann also presented an empirical expression that gives an

accurate representation, if the range of wavelength is not too large,

$$n = n_0 + b/(\lambda - \lambda_0) \quad (9)$$

where n_0 , λ_0 , and b are constants to be determined from the observations.

(2) When the refracting material shows selective absorption in the range of wavelengths with one or more absorption bands, the above expressions are too restrictive. As an absorption band in the neighborhood of the absorption wavelength is approached from the short-wavelength side, the index of refraction decreases more rapidly than the Cauchy or Hartmann formula can account for. On the long-wavelength side of the absorption band the refractive index is high and decreases rapidly. As the wavelength further increases the curve takes on a form which is again represented approximately by a Cauchy or Hartmann formula with a new set of constants. Within the band it is extremely difficult to obtain experimental data.

In 1871 Sellmeier found a semi-empirical equation,

$$n^2 = 1 + \sum_{j=1}^N A_j \lambda^2 / (\lambda^2 - \lambda_j^2) \quad (10)$$

where λ is the wavelength of the incident light; λ_j is the j th of N absorption wavelengths for the medium and A_j a corresponding constant.

Sellmeier's derivation was based on an elastic-solid theory in which he supposed that the frictionless particles of the medium were subjected to elastic forces and possessed natural frequencies of vibration. The effect of a light wave travelling through the medium was to impress a periodic oscillating force, so that the frictionless particles took up the motion characteristic of a forced vibration.

For $\lambda = 0$, the curve starts at value $n = 1$. As λ increases,

the curve falls, approaching a value of $n = -\infty$ at resonance. On the long-wavelength side of the absorption band the refractive index has an abnormally large value, being infinite at resonant wavelength. The refractive index again approaches a large value toward $-\infty$ as λ approaches the second natural frequency. Sellmeier's equation is thus successful in explaining the "anomalous" variation of n , i.e. larger values of the index at longer wavelengths than for some shorter wavelengths in the neighborhood of an absorption frequency. However since n becomes $-\infty$ as λ approaches λ_j from the short-wavelength side and n becomes $+\infty$ as λ approaches λ_j from the long-wavelength side, Sellmeier's equation cannot represent the dispersion very close to an absorption band.

(3) The failure of Sellmeier's equation in the absorption band is due to the fact that the frictional resistance is neglected. Kettler and Helmholtz added friction to the mechanical oscillators in the elastic medium postulating that as they vibrate they experience a frictional resistance the effect of which increases as the frequency of the wave approaches the natural frequency of an oscillator. Thus the absorption of energy in the wave is accounted for (15).

(4) With the development of Maxwell's electromagnetic theory and the electron theory of Lorentz (16) and Drude (15) the mechanical vibrator was replaced by an atomic dipole which is made to undergo forced vibrations and is subject to resistances that are proportional to velocity.

Consideration of the frequency dependence of polarization resulting from the elastic displacements leads to the equation for a gas (17):

$$(n - ik)^2 = 1 + 4\pi \sum_j N_j (e_j^2 / m_j) / (\omega_j^2 - \omega^2 + i\omega g_j) \quad (11)$$

where N_j is the number of oscillators of the j th kind per unit volume corresponding to the natural angular velocities ω_j and the damping constant g_j which determines the magnitude of the frictional forces acting, e_j and m_j are the corresponding charge and mass of the oscillators, and ω is the angular velocity of the light wave. The term $(n - ik)$ is complex with n the refractive index and k the extinction coefficient. Substituting $2\pi c/\lambda_j$ for ω_j and $2\pi c/\lambda$ for ω the complex index of refraction may be written as

$$(n - ik)^2 = 1 + \sum_j A_j \lambda^2 / (\lambda^2 - \lambda_j^2 + iG_j \lambda) \quad (12)$$

where $A_j = N_j e_j^2 \lambda_j^2 / \pi m_j c^2$ and

$$G_j = \lambda_j^2 g_j / 2\pi c.$$

Separating the real and the imaginary parts lead to the two equations

$$n^2 - k^2 = 1 + \sum_j A_j \lambda^2 (\lambda^2 - \lambda_j^2) / [(\lambda^2 - \lambda_j^2)^2 + G_j^2 \lambda^2] \quad (13)$$

and

$$2nk = \sum_j A_j G_j \lambda^3 / [(\lambda^2 - \lambda_j^2)^2 + G_j^2 \lambda^2]. \quad (14)$$

The extinction coefficient is related (14) to the coefficient of absorption α by the relation

$$k = (\lambda / 4\pi) \alpha. \quad (15)$$

In solids, assuming the internal field is given by Lorentz, the complex refractive index becomes for a similar one-dimensional treatment (17):

$$(n - ik)^2 = 1 + 4\pi \sum_j N_j (e_j^2 / m_j) / (\omega_j^2 - \omega^2 + ig_j \omega - 4\pi N_j e_j^2 / 3m_j) \quad (16)$$

In place of ω_j^2 there appears the quantity

$$\omega_j^2 - (4\pi/3) N_j (e_j^2/m_j) \quad (17)$$

that is, the absorption frequency is displaced.

(5) Nozieres and Pines (18) have developed a quantum theory of the dielectric constant for solids of both low and high polarizability from first principles. In the latter case, the approach used is collective in that the long-range part of the electron interaction is described by the plasmon (a quantized collective plasma oscillation of the electron gas) field. They conclude that for highly polarizable solids the above type of local field correction is unimportant. Local field corrections could be necessary in low polarizability regions but then they represent a small correction. Consequently a simpler expression such as that given in equation (12) may well represent the general experimental results. As will be seen later, the mathematical form of this Kettler-Helmholtz relation provides a good fit to the measured index of refraction values reported here.

CHAPTER III

DISPERSION MEASUREMENT

Cutting and Polishing of the Prism

The cassiterite ore crystal from which the prism was cut came from Araca, Bolivia. It was a twin of very dark brown appearance, and in size was approximately 1.5 x 1.5 x 2.5 cm. The sample was glued to the Bridgeport vertical milling machine with Canada balsam and the twin was separated along the twinning plane with a 0.03 by 3.0 inch circular diamond saw.

The smaller of the two separated pieces was used to determine the optic axis while the larger piece was saved for making the prism.

The approximate direction of the optic axis was first determined by studying the various facial angles of the crystal and then thin sections of less than 1.0 mm in thickness were cut perpendicular to the approximately determined optic axis with the above diamond saw. Each thin section was placed on the stage of a Leitz polarizing microscope. A trial and error method was employed--in other words, various thin sections were cut at different angles to the roughly determined direction of optic axis and they were studied under the polarizing microscope until one was found to have a black cross superimposed on concentric circles of interference colors as shown in Figure 13.

Convergent polarized light passing through an anisotropic thin

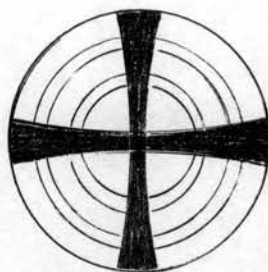


Figure 13

A Uniaxial Interference Figure Looking Down An Optic Axis

crystal section yields a range in retardation between crossed nicols (19). In hexagonal and tetragonal crystals the optic axis is also the c-axis of the crystal. Hence, the center of the black cross in the interference figure indicated the optic axis direction. If the optic axis of the crystal coincides with that of the microscope, the uniaxial figure will be centered with the two arms crossing at the intersection of the crosshairs in the microscope.

If the optic axis is not along the axis of the microscope, the point of intersection of the cross arms will not coincide with the intersection of the crosshairs and may even fall outside the field of the microscope. If the center of the axial cross does not coincide with the center of the field, the point of intersection of the arms will move around the crosshair intersection when the stage is rotated. A circle will be described when the stage is rotated 360° . The intersection of the cross arms marks the point of emergence of the optic axis. The deviation from the center of the field is a measure of the angle of deviation between the optic axis and the axis of the polarizing microscope.

After the optic axis of the smaller half of the twin was accurately

determined with the above method, a prism with its optic axis along its refracting edge was prepared from the larger half of the twin.

The polishing of the prism consisted of three stages: first of all the prism was polished on 320 wet or dry 3M carbonrundum paper, second it was polished on glass plate with American Optical compound N303 in water until a mud finish was obtained, and the last step was to polish the prism on a piece of blotter paper impregnated with Linde grade A polishing compound.

The finished prism had a refracting angle of $20^{\circ} 56.5'$ and the following approximate dimensions:

Edge = 5.94 mm

Width of base = 6.27 mm

Height (from base to vertex) = 16.15 mm

The prism was surprisingly transparent with a light brown color as compared to very dark brown before it was polished. A dark streak was observed near the base of the prism and a small reddish spot near the refracting angle.

Experimental Procedure

The experimental procedure of the dispersion measurements followed very closely that of Pfund (20). A schematic diagram of the design of the mirror spectrograph used in this work is shown in Figure 14. A light-tight, circulating air-cooled spectral lamp housing H was built with an adjustable slit S. The radiation from the spectral lamp was allowed to proceed through the slit to a mounted front-surfaced concave mirror A (15 cm focal length, 10 cm diameter) which provided parallel rays through the cassiterite prism C, placed on a divided circle mounted on a heavy

tripod stand. Light then passed to the second mounted front-surface concave mirror B (100 cm focal length, 10 cm diameter) which, finally, projected both the ordinary and the extraordinary spectrum on a photographic plate P.

The lamp housing and the first concave mirror were mounted on a single optical bench. The second concave mirror and the camera were mounted on another optical bench. The slit was set at the focal point of the first concave mirror, the photographic plate was set at the focal point of the second mirror. The focusing of the spectral lines was done by means of a 9X eyepiece set behind the camera. Focusing with ground glass was found to be inadequate because of the large amount of scattered radiation from the mirror. A long metal tubing was set in front of the camera and was extended to as close to the second concave mirror as possible so as to cut down the scattered radiation from falling on the photographic plate. However, this tube had to be short enough so that it did not block the spectrum coming through the prism to the second concave mirror.

Additional dispersion measurements were made in the visible range with a conventional telescope spectrometer accurate to 20 seconds. The following sources were used in connection with this spectrometer: hydrogen, helium, sodium, mercury, cadmium, cesium, rubidium and thallium. The range of visible wavelengths observed was from 435.8 millimicrons to 667.8 millimicrons.

Derivation of the Formula Used in Calculating the Refractive Indices with Data Obtained by the Mirror Spectrograph

Dispersion measurements in the near infra red and the ultraviolet

required the use of the mirror spectrograph. By means of the standard spectrometer the refractive angle of the prism A was found and the angles of minimum deviation D for the mercury 546.1 mμ line was determined visually both for the ordinary ray and the extraordinary ray. From these measurements the refractive indices, both ordinary and extraordinary, were calculated in the conventional manner. The prism was then mounted to form part of the mirror spectrograph as shown in Figure 14. The prism was then adjusted to minimum deviation for the ordinary 546.1 line before the ordinary spectrum was photographed, and it was reset at minimum deviation for the extraordinary 546.1 line when the extraordinary spectrum was photographed.

Consider photographing the ordinary spectrum: (the formula to be derived also applies to the extraordinary spectrum as long as the minimum deviation is set for the extraordinary 546.1 line).

The prism was adjusted to minimum deviation for the ordinary 546.1 line. All other wavelengths passed through the prism at angles other than minimum deviation - for example, the radiation of wavelength 435.8 mμ followed the ray path shown in Figure 15.

For $\lambda = 435.8 \text{ m}\mu$, one obtains from Snell's law

$$\sin i_1 / \sin r_1 = \sin i_2 / \sin r_2 \quad (19)$$

$$\sin r_2 = \sin i_2 \sin r_1 / \sin i_1 \quad (20)$$

again $r_1 + r_2 = A$, hence $r_2 = A - r_1$.

Expanding:

$$\begin{aligned} \sin r_2 &= \sin (A - r_1) \\ &= \sin A \cos r_1 - \cos A \sin r_1 . \end{aligned} \quad (21)$$

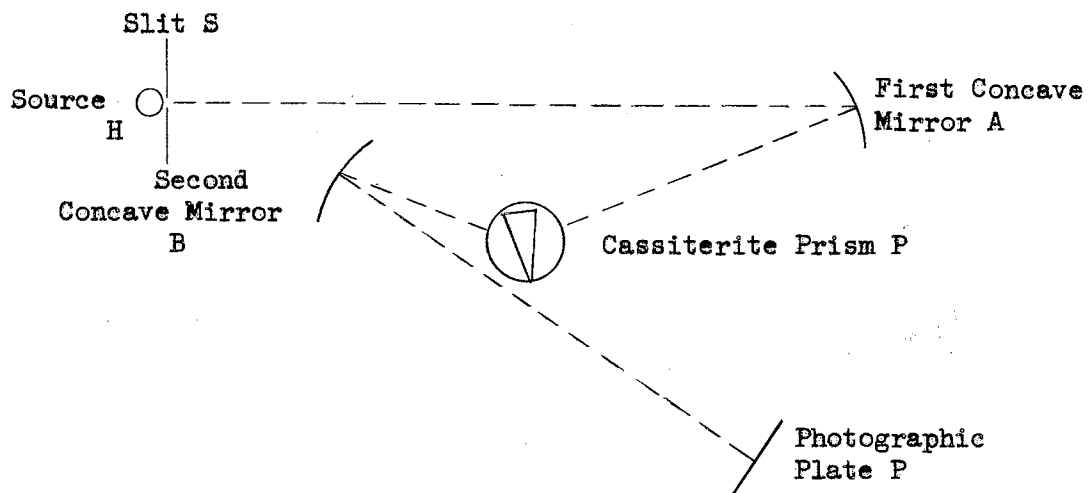


Figure 14

Schematic Diagram of the Mirror Spectrograph

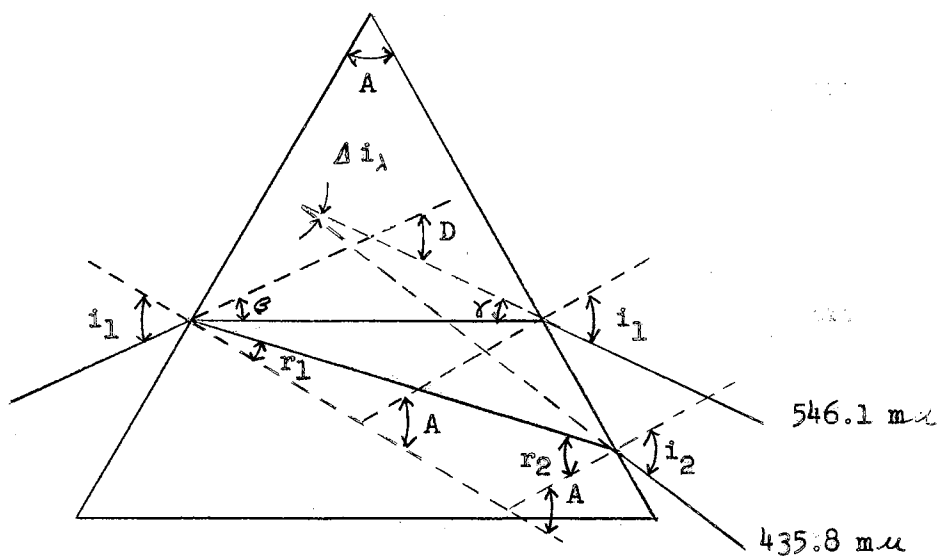


Figure 15

Ray Diagram

Equating (20) and (21)

$$\sin A \cos r_1 - \cos A \sin r_1 = \sin i_2 \sin r_1 / \sin i_1$$

$$\sin i_1 \sin A \cos r_1 - \sin i_1 \cos A \sin r_1 = \sin i_2 \sin r_1$$

$$\sin i_2 \sin r_1 + \sin i_1 \cos A \sin r_1 = \sin i_1 \sin A \cos r_1$$

$$\sin r_1 (\sin i_2 + \sin i_1 \cos A) = \sin i_1 \sin A \cos r_1$$

$$\sin r_1 / \cos r_1 = \tan r_1 = \sin i_1 \sin A / [(\sin i_1 \cos A) + \sin i_2]$$

$$r_1 = \tan^{-1} (\sin i_1 \sin A / (\sin i_1 \cos A + \sin i_2)). \quad (22)$$

Whence, finally

$$n_{435.8} = \sin i_1 / \sin r_1 \quad (23)$$

This is the working equation with r_1 given by equation (22).

At minimum deviation the refracted ray inside the prism makes equal angles with the two prism faces.

In this special case,

$$i_1 = i_2 \quad (24)$$

$$r_1 = r_2 \quad (25)$$

$$\beta = \delta \quad (26)$$

The exterior angle D equals the sum of the opposite interior angles $\beta + \delta$. Similarly, the exterior angle A equals the sum $r_1 + r_2$.

Consequently,

$$A = 2r_1 \quad (27)$$

$$D = 2\beta \quad (28)$$

$$i_1 = r_1 + \beta \quad (29)$$

Solving equations (27), (28) and (29) for r_1 and i_1

$$r_1 = \frac{1}{2} A \quad (30)$$

$$\beta = \frac{1}{2} D \quad (31)$$

$$i = \frac{1}{2} (A + D) \text{ (same for all wavelengths).} \quad (32)$$

Consequently, when the prism was set for minimum deviation for the 546.1 line and the angle D previously determined by the standard spectrometer, the angle i, needed in the working equation was fixed by the above expression.

Since by Snell's law

$$n = \sin i_1 / \sin r_1 \quad (33)$$

$$n_{\text{min. dev. } \lambda} = \sin \frac{1}{2}(A + D) / \sin \frac{1}{2}A \quad (34)$$

This, of course, is the standard spectrometer working equation used for visible measurements.

The angle of incidence i_1 equals the angle of emergence i_2 only for the 546.1 line. For other lines

$$i_2 = i_1 \pm \Delta i_\lambda \quad (35)$$

where $\Delta i_\lambda = \Delta l_\lambda / F$ in radians. (36)

Δl_λ is the linear separation on the photographic plate of the various spectral lines measured from the 546.1 line. F is the focal length of the second concave mirror. With determination of Δi_λ to give the i_2 needed in equation (22), all the necessary information to calculate the index of refraction for any wavelength line is available. For sources other than mercury the prism was set for minimum deviation of other convenient bright lines in the visible range. These wavelengths are

indicated by asterisks in Table II.

Description of Spectroscopic Plates

Kodak Royal Pan film, $3\frac{1}{4} \times 4\frac{1}{4}$ inch, was used first for testing the alignment of the mirror spectrograph. Kodak spectroscopic plates were used for the actual photographing of the spectral lines.

Kodak spectroscopic plate (21) emulsion type 103 is an emulsion of high light-sensitivity, medium contrast, fine granularity and of moderately low resolving power, between 60 and 70 lines per mm. Emulsion type I (Infrared) is an emulsion of high sensitivity, high contrast, and fine granularity.

Class F spectral sensitivity has very uniform sensitization for the whole visible spectrum, especially for the red to $680 \text{ m}\mu$. This type of plates must be handled in total darkness. Class N spectral sensitivity has very uniform sensitivity from 600 to $860 \text{ m}\mu$.

The recommended tray development time at 20°C using Kodak D-19 developer is 4 minutes with continuous agitation. After development, the plate should be rinsed with agitation in running water at 18° to 21°C for 30 seconds, and then fixed for 10 to 20 minutes at 18° to 21°C with Kodak Acid Fixer or Kodak Fixing Bath F-5, or 3 to 5 minutes with Kodak Rapid Fixer or Kodak Rapid Fixing Bath F-7. The plates should be agitated frequently during fixing.

Processing is completed by washing for 20 to 30 minutes in running water and then drying in a dust free place.

Table I shows the exposure time with different types and classes of plates used and the different spectral lamps used in the mirror spectrograph.

In order to prevent over-exposing of the strong visible lines of mercury, a filter was set in front of the slit so that lines close to the absorption edge could be brought out more clearly.

TABLE I
EXPOSURE TIME

Source (Osram)	Plates	Exposure Time in Sec. Without Filter	Exposure Time in Sec. With Filter
Hg	103-F	10	120 w/Corning CS7-51
Cd	103-F	30	
Cd	103-F	120 (To bring out 361.1 m μ line)	
Tl	103-F	20	
Cd	I-N	25	

CHAPTER IV

RESULT OF MEASUREMENT AND ITS ACCURACY

The result of dispersion measurements, both for the ordinary and the extraordinary rays, are tabulated in Table II. In column one of Table II are the sources of radiation; these are spectral lamps made by Osram. In column two are the wavelengths of the utilized persistent lines of the various sources, these values taken from the Handbook of Chemistry and Physics (22). Column three gives the ordinary and the extraordinary refractive indices of the cassiterite prism as measured by a Gaertner spectrometer. The refractive indices measured by the mirror spectrograph are given in column four. Columns five and six are the values of refractive indices calculated by the use of Ecklebe's first and second formulas respectively (9).

By means of the Gaertner spectrometer the angles were determined with a maximum error of setting of ± 20 seconds which introduced an uncertainty of ± 0.0006 in the value of index of refraction. By means of a measuring microscope the positions of the lines on the spectroscopic plate were determined with a maximum error of setting of ± 0.005 cm. The calculation of the index of refraction using equation (23) requires the knowledge of the value of the angle of incidence of a visible line which is set for minimum deviation as was shown in equation (32). For photographing the mercury lines for example, the $546.1 \text{ m}\mu$ line of mercury was set at minimum deviation and the angle of minimum deviation D and the

TABLE II
REFRACTIVE INDICES

Source	Wavelength ($m\mu$)	Gaertner Spectrometer		Mirror Spectrograph		Ecklebe's 1st. Formula		Ecklebe's 2nd. Formula
		n_o	n_e	n'_o	n'_e	n''_o	n''_e	n'''_o
Cd	361.0	--	--	2.0987	--	2.1075	--	2.1112
Hg	365.0	--	--	2.1038	--	2.1035	--	2.1066
Tl	377.5	--	--	2.0842	--	2.0915	--	2.0936
Hg	404.7	--	--	2.0664	2.1627	2.0700	2.1597	2.0705
Hg	435.8	2.0490	2.1444	2.0463	2.1414	2.0509	2.1427	2.0506
He	447.1	2.0427	2.1355	--	--	2.0451	2.1374	2.0446
Cs	455.5	2.0401	2.1315	--	--	2.0411	2.1338	2.0405
Cs	459.5	2.0363	2.1278	--	--	2.0393	2.1322	2.0387
Cd	467.8	2.0330	2.1248	2.0306	2.1254	2.0359	2.1290	2.0350
Cd	480.0	2.0278	2.1204	2.0262	2.1219	2.0308	2.1245	2.0301
H	486.1	2.0267	2.1201	--	--	2.0285	2.1224	2.0278
He	501.6	2.0211	2.1153	--	--	2.0230	2.1175	2.0223
Cd*	508.6	2.0174	2.1116	--	--	2.0208	2.1154	2.0200
Tl*	535.0	2.0104	2.1045	--	--	2.0130	2.1085	2.0124
Rb	543.2	2.0077	--	--	--	2.0110	2.1065	2.0104
Hg*	546.1	2.0062	2.1016	--	--	2.0102	2.1059	2.0096
Rb	572.4	2.0014	2.0971	--	--	2.0041	2.1003	2.0036
Hg	577.0	1.9990	2.0960	1.9985	2.0946	2.0031	2.0994	2.0027
Cs	584.4	1.9984	2.0953	--	--	2.0016	2.0981	2.0012
He	587.6	1.9980	2.0950	--	--	2.0010	2.0975	2.0006
Na	590.0	1.9976	2.0935	--	--	2.0005	2.0971	2.0002
Cs	603.4	1.9950	2.0916	--	--	1.9980	2.0948	1.9977
Cs	621.3	1.9916	2.0891	--	--	1.9949	2.0919	1.9947
Rb	629.8	1.9910	2.0883	--	--	1.9935	2.0907	1.9934
Cd	643.8	1.9883	2.0850	1.9920	2.0850	1.9914	2.0887	1.9914
H	656.3	1.9876	2.0830	--	--	1.9896	2.0871	1.9897
He	667.8	1.9856	2.0823	--	--	1.9881	2.0856	1.9882
Cd	738.4	--	--	1.9789	2.0708	1.9802	2.0784	1.9808

refractive angle A of the prism were determined by the use of the Gaertner spectrometer which introduced a maximum error of setting for each of ± 20 seconds. In addition, taking into account the maximum error of setting ± 0.005 cm when the positions of lines were measured, gave a total uncertainty of measurement for the mirror spectrograph of ± 0.0019 in the value of n . These limits do not take into account the possibility of such factors as misalignment of the mirror spectrograph. However, it is evident from Table III that the dispersion measurements taken with the standard spectrometer and those taken with the mirror spectrograph agree within less than a factor of 1.5 of the above predicted experimental error and show no systematic bias.

Ecklebe's first formula and second formula are those of Kettler-Helmholtz (15):

$$\text{Formula 1: } n^2 = 1 + m' \lambda^2 / (\lambda^2 - \lambda_v^2)$$

$$\text{Formula 2: } n^2 = m + \left[m_v \lambda^2 / (\lambda^2 - \lambda_v^2) \right] + \left[m_r \lambda^2 / (\lambda^2 - \lambda_r^2) \right]$$

The empirical constants calculated by Ecklebe for Formula 1 are:

Ordinary

$$m' = 2.7886$$

$$\lambda_v = 157.3 \text{ m}\mu$$

Extraordinary

$$m' = 3.1912$$

$$\lambda_v = 145.4 \text{ m}\mu$$

and the constants for Formula 2 for the ordinary ray are:

$$\lambda_v = 186.1 \text{ m}\mu$$

$$\lambda_r = 1134.2 \text{ m}\mu$$

$$m = 1.98349$$

$$m_v = 1.81642$$

$$m_r = 0.0008444$$

The more complex form of Formula 2 is designed to give

TABLE III

RELATIVE DIFFERENCES OF THE REFRACTIVE INDICES*

Source	Wavelength (μm)	$n_o - n'_o$	$n_e - n'_e$	$n_o - n''_o$	$n_e - n''_e$	$n_o - n'''_o$	$n'_o - n''_o$
Cd	361.0	-	-	-	-	-	-0.0125
Hg	365.0	-	-	-	-	-	-0.0031
Tl	377.5	-	-	-	-	-	-0.0094
Hg	404.7	-	-	-	-	-	-0.0041
Hg	435.8	+0.0027	+0.0030	-0.0019	+0.0017	-0.0016	-0.0043
He	447.1	-	-	-0.0024	-0.0019	-0.0019	-
Cs	455.5	-	-	-0.0010	-0.0023	-0.0004	-
Cs	459.5	-	-	-0.0030	-0.0044	-0.0024	-
Cd	467.8	+0.0024	-0.0006	-0.0029	-0.0042	-0.0020	-0.0044
Cd	480.0	+0.0016	-0.0015	-0.0030	-0.0041	-0.0023	-0.0039
H	486.1	-	-	-0.0018	-0.0023	-0.0011	-
He	501.6	-	-	-0.0019	-0.0022	-0.0012	-
Cd	508.6	-	-	-0.0034	-0.0038	-0.0026	-
Tl	535.0	-	-	-0.0026	-0.0040	-0.0020	-
Rb	543.2	-	-	-0.0033	-	-0.0027	-
Hg	546.1	-	-	-0.0040	-0.0043	-0.0034	-
Rb	572.4	-	-	-0.0027	-0.0032	-0.0022	-
Hg	577.0	+0.0005	+0.0014	-0.0041	-0.0034	-0.0037	-0.0042
Cs	584.4	-	-	-0.0032	-0.0028	-0.0028	-
He	587.6	-	-	-0.0030	-0.0025	-0.0026	-
Na	590.0	-	-	-0.0029	-0.0036	-0.0026	-
Cs	603.4	-	-	-0.0030	-0.0032	-0.0027	-
Cs	621.3	-	-	-0.0033	-0.0028	-0.0031	-
Rb	629.8	-	-	-0.0025	-0.0024	-0.0024	-
Cd	643.8	-0.0037	-0.0000	-0.0031	-0.0037	-0.0031	+0.0006
H	656.3	-	-	-0.0020	-0.0041	-0.0020	-
He	667.8	-	-	-0.0025	-0.0033	-0.0024	-
Cd	738.4	-	-	-	-	-	-0.0019

*See Table II for meaning of symbols.

consideration to the effect of infrared absorption. However, this provides little correction and it is to be noted that the third term was not used in calculating the index of refraction n''_o as given in Table II because this term would give values only in the sixth and seventh decimals. The measured values of index of refraction and those calculated by the use of Ecklebe's second formula in general agreed within less than 0.20 per cent of each other. However, the differences in the ultraviolet range are as high as 0.6 per cent which is not surprising because the formula was fitted for the range of wavelengths from 444.0 to 715.2 $m\mu$. Actually there is little choice to be made between the two formula representations except that a slightly better fit is afforded by Formula 2 in the middle of the wavelength range.

Considering the instrument accuracies of the Gaertner spectrometer and the mirror spectrograph, the imperfections in the planarity of the prism faces, and the different impurity contents of the natural cassiterite used for the prism, Ecklebe's formulas are judged for all practical purposes to be suitable for fitting the dispersion measurements of the author's cassiterite prism and hence no additional empirical fitting of the experimental values of indices of refraction was carried out. There is a systematic small negative difference between the present results and those of Ecklebe but in view of the factors mentioned above it is considered relatively unimportant for interpretation at this time.

The dispersion curves for the ordinary ray and extraordinary ray are shown in Figure 16.

It should be noted that the values of index of refraction for the extraordinary ray for the wavelengths of 377.5, 365.0 and 361.0 $m\mu$ are missing in Table II. Exposure times of the order of 10 to 50 times

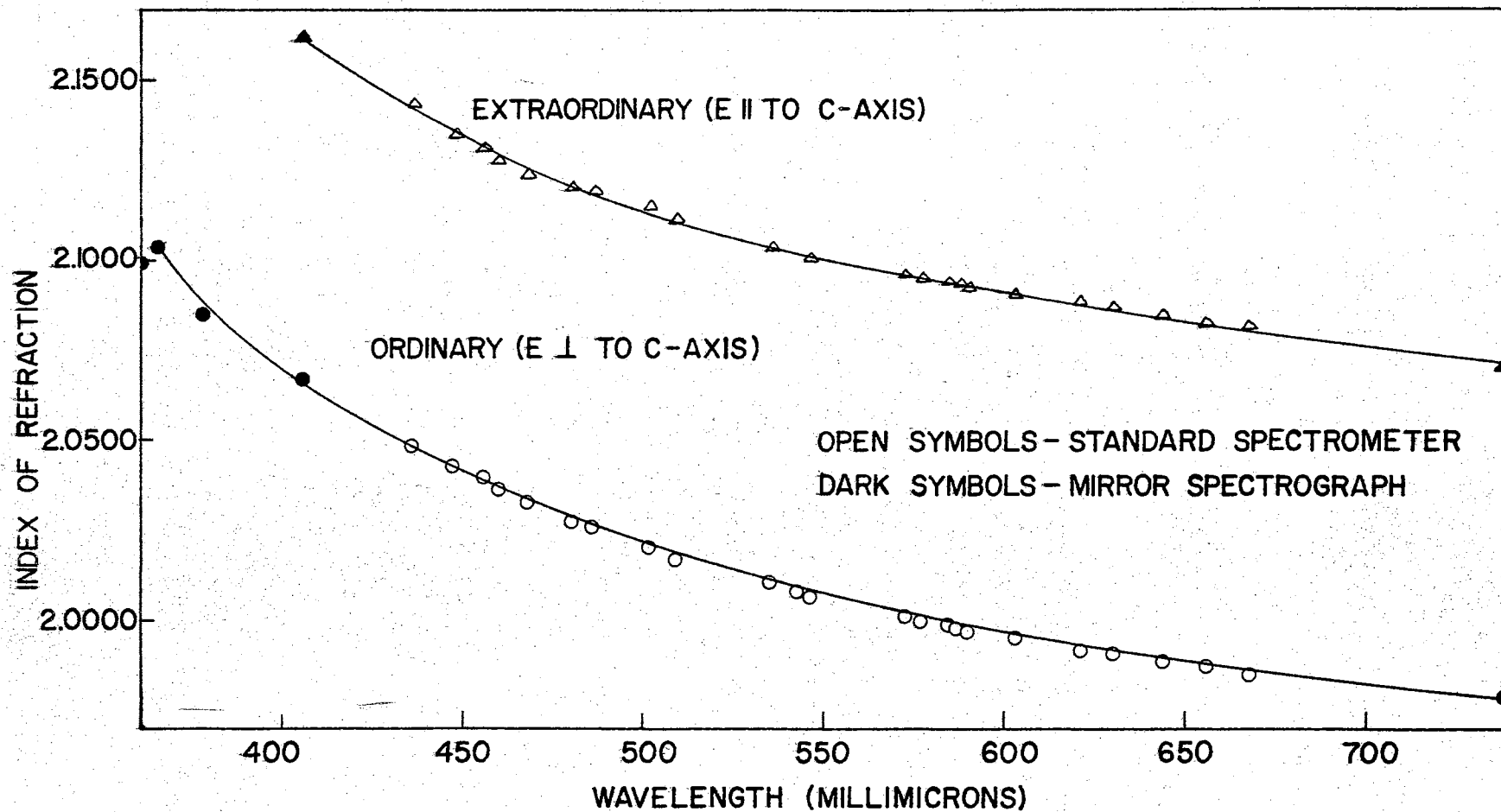


FIGURE 16. DISPERSION CURVE

longer than those usually required to bring out the same lines in the ordinary spectrum failed to produce any sign of the extraordinary lines. This is an indication of dichroism with the absorption of the extraordinary ray greater than that of the ordinary. However, the magnitude of the effect is difficult to judge since these wavelengths are near the transmission edge and the extraordinary ray path length in the material is greater than that of the ordinary ray.

CHAPTER V

SUMMARY AND CONCLUSIONS

Brief Summary of the Work

A small piece of natural stannic oxide (cassiterite) ore was obtained from Araca, Bolivia. It was noticed that the crystal was a twin. The twin was sawed into two pieces along the twinning plane by gluing it to a Bridgeport vertical milling machine with Canada balsam and cutting with a 0.03 inch circular diamond saw. The optic axis of the sample was roughly determined first from its facial angles and then thin sections were cut off and placed on the stage of a polarizing microscope, allowing the optic axis to be determined with accuracy from the interference figure.

A small prism with optic axis along its refracting edge was then cut and polished. Dispersion measurements were made both with a standard spectrometer and a mirror spectrograph. The Gaertner spectrometer had a maximum error of setting of ± 20 seconds which introduced an uncertainty of ± 0.0006 in the value of the index of refraction. The mirror spectrograph used essentially consisted of a spectral lamp whose radiation was allowed to pass through a slit to a front-surfaced concave mirror which provided parallel radiation through the prism to a second front-surfaced concave mirror which in turn finally projected the resultant ordinary and extraordinary spectra on a photographic plate where they appeared side by

side.

The prism was set at minimum deviation of a known wavelength whose angle of minimum deviation could be predetermined with the Gaertner spectrometer. With this angle of minimum deviation known and with the angle of the prism, also known, the focal length of the second concave mirror and the relative separations of different spectral lines on the photographic plate provided enough information so that the indices of refraction of the ordinary and the extraordinary rays could be calculated.

The positions of the lines on the plate were measured with a measuring microscope which had a maximum error of setting of ± 0.005 cm and this coupled with the uncertainty of the angle of the prism and the angle of minimum deviation introduced a maximum uncertainty in the indices of refraction calculated by the use of the spectrograph of ± 0.0019 .

Kodak spectroscopic plates with spectral sensitivity ranges from 250 to 800 $m\mu$ were used.

The photographic method used allowed extension of dispersion measurements to both shorter and longer wavelengths than those reported by Ecklebe (9).

Conclusions

Dispersion measurements made by the Gaertner spectrometer and those made by the mirror spectrograph agreed with each other within less than 0.2%. The per cent difference between the measured values and those calculated with the use of Ecklebe's empirical formula of the Kettler-Holmholtz type is less than 0.20 in the visible range and about 0.6 in the ultraviolet. The larger per cent difference in the ultraviolet is

not surprising since Ecklebe determined his constants with dispersion measurements only in the range from 423.1 to 715.2 $m\mu$.

The apparently anomalous variation of the two shortest wavelength points in the ordinary ray dispersion curve from values predicted by the simple empirical formula was verified by a number of independent measurements. This may mean that the extinction coefficient (k) term is becoming important since the absorption is rapidly increasing in this wavelength range. Additional information from absorption and reflection measurements needs to be obtained to check this possibility.

No empirical fitting of the equation of dispersion was carried out since Ecklebe's expression was considered to be adequate for practical purposes in fitting the dispersion measurements of the cassiterite prism prepared by the author.

Dichroism was observed in cassiterite, with absorption of the extraordinary ray greater than that of the ordinary ray. Three lines with wavelengths of 377.5, 365.0, 361.0 $m\mu$ showed up very nicely in the ordinary spectrum while exposure times of the order of 10 to 50 times longer than those required to bring out the above lines failed to bring out the extraordinary lines.

Suggestions for Further Study

As soon as large synthetic single crystals of cassiterite are available, a larger prism should be cut with the optic axis in the refracting edge and a comparable set of dispersion measurements made.

An iron-arc should be constructed to be used with the mirror spectrograph in order that more lines in the range of wavelength from 360 to 440 $m\mu$ may be obtained. Dispersion measurements should also be

extended to wavelengths above 1μ although it necessitates a modification of the present mirror spectrograph used by the author. This would require a very long focal length concave mirror in order to additionally separate the lines in the near infrared for precise measurement. Also needed would be a stronger source of radiation and a wider spectroscopic plate of extended sensitivity range.

An extensive study of the dichroism in cassiterite near the absorption edge should be made using transmission techniques.

The experimental curves should be examined in the light of dispersion theory in order to gain new insight into the microscopic properties of stannic oxide.

BIBLIOGRAPHY

1. Northrip, J. W. II. Master's Thesis, Oklahoma State University, 1958 (Unpublished). Pertinent excerpts found in Annual Summary Report (1959), Office of Naval Research Contract No. Nonr-2595(01).
2. Hurt, J. E. Master's Thesis, Oklahoma State University, 1959 (Unpublished). Included as an Appendix in Annual Summary Report (1959), Office of Naval Research Contract No. Nonr-2595(01).
3. Belski, A. J. Master's Thesis, Oklahoma State University, 1960 (Unpublished). Included as Part I in Annual Summary Report (1960), Office of Naval Research Contract No. Nonr-2595(01).
4. Tolly, E. E. Master's Thesis, Oklahoma State University, 1962 (unpublished). Included as Section I in Annual Summary Report (1961), Office of Naval Research Contract No. Nonr-2595(01).
5. Houston, J. E. Master's Report, Oklahoma State University, 1962 (Unpublished). Included as Section B in Annual Summary Report (1962), Office of Naval Research Contract No. Nonr-2595(01).
6. Kunkle, H. F. Master's Report, Oklahoma State University, 1961 (Unpublished). Included as an Appendix in Annual Summary Report (1961), Office of Naval Research Contract No. Nonr-2595(01).
7. Marley, J. A., MacAvoy, T. C. "Growth of Stannic Oxide Crystals from the Vapor Phase." J. Appl. Phys., 32, 12 (1961).
8. Kohnke, E. E., "Electrical and Optical Properties of Natural Stannic Oxide Crystals." J. Phys. Chem. Solids (In Press, 1962).
9. Ecklebe, F. "Optical Studies on Cassiterite in the Temperature Region 16-1100°C." Neus Jahrb. Mineral. Geol., Beil Bd. 66A, 47-88 (1933).
10. Palache, C., Berman, H., Frondel, C. "Cassiterite." Dana's System of Mineralogy, New York: John Wiley & Sons, Inc., 1944, pp. 574-581.
11. Hurlbut, C. S. Jr. Dana's Manual of Mineralogy. New York: John Wiley and Sons, Inc. 1959.
12. Buerger, M. J. Elementary Crystallography. New York: John Wiley and Sons, Inc., 1956.

13. Morgan, J. Introduction to Geometrical and Physical Optics. New York: McGraw Hill Book Company, Inc., 1953.
14. Andrews, C. L. Optics of the Electromagnetic Spectrum. New Jersey: Prentice-Hall, Inc., 1960.
15. Drude, P. The Theory of Optics. New York: Dover Publications, Inc., 1959.
16. Lorentz, H. A. The Theory of Electrons. Leipzig: Teubner, 1909.
17. Dekker, A. J. Solid State Physics. New Jersey: Prentice-Hall, Inc., 1957.
18. Nozieres, P., Pines, D. "Electron Interaction in Solids. Collective Approach to the Dielectric Constant." Phys. Rev. 109, 3 (1958).
19. Kerr, P. F., Optical Mineralogy. 3rd. ed. New York: McGraw-Hill Book Company, Inc., 1959.
20. Pfund, A. H. "The Dispersion and Transmission of Methyl Methacrylate Polymer." J. Opt. Soc. Am. 29, 291 (1939).
21. Kodak Photographic Films and Plates for Scientific and Technical Use. 8th. ed. New York: Eastman Kodak Company, 1960.
22. Hodgman, C. D., ed. Handbook of Chemistry and Physics. 32nd. ed. Ohio: Chemical Rubber Publishing Co., 1950.

VITA

Steiner Sei-Hwa Huang

Candidate for the Degree of

Master of Science

Thesis: REFRACTIVE INDICES OF CASSITERITE

Major Field: Physics

Biographical:

Personal Data: Born at Amoy, Fukien, China, May 5, 1935, the son of Mr. & Mrs. Oei Tjoe.

Education: Attended primary school in Shanghai, Kiangsu and Amoy, Fukien, China; graduated from St. Stephen's Boys' College, a high school in Hong Kong, in 1954. Attended Chung Chi College, Hong Kong, from 1954 until January, 1955; received the Bachelor of Science degree from the University of Wyoming, Laramie, Wyoming, with a major in Electrical Engineering in May 1958 and at the same time completed all requirements for a Bachelor of Science degree in Mathematics. Attended graduate school at Colorado University, Boulder, Colorado in the summer, 1959 and attended Kansas State University, Manhattan, Kansas, in summer, 1961; completed requirements for the Master of Science degree in February, 1963.

Experience: Employed for two years as an instructor of physics at Northeastern State College, Tahlequah, Oklahoma.

Organizations: Member of Sigma Pi Sigma, American Association of Physics Teachers, Institute of Radio Engineers and American Institute of Electrical Engineers.